Anal Bioanal Chem (2014) 406:6963–6977
DOI 10.1007/s00216-014-8143-7

TRENDS

Trends in single-cell analysis by use of ICP-MS

Larissa Mueller · Heike Traub · Norbert Jakubowski · Daniela Drescher · Vladimir I. Baranov · Janina Kneipp

Received: 5 June 2014 / Revised: 14 August 2014 / Accepted: 28 August 2014 / Published online: 1 October 2014

Abstract The analysis of single cells is a growing research field in many disciplines such as toxicology, medical diagnosis, drug and cancer research or metallomics, and different methods based on microscopic, mass spectrometric, and spectroscopic techniques are under investigation. This review focuses on the most recent trends in which inductively coupled plasma mass spectrometry (ICP-MS) and ICP optical emission spectrometry (ICP-OES) are applied for single-cell analysis using metal atoms being intrinsically present in cells, taken up by cells (e.g., nanoparticles), or which are artificially bound to a cell. For the latter, especially element tagged antibodies are of high interest and are discussed in the review. The application of different sample introduction systems for liquid analysis (pneumatic nebulization, droplet generation) and elemental imaging by laser ablation ICP-MS (LA-ICP-MS) of single cells are highlighted. Because of the high complexity of biological systems and for a better understanding of processes and dynamics of biologically or medically relevant cells, the authors discuss the idea of "multimodal spectroscopies."

Keywords Bioanalytical methods · Cell systems/single cell analysis · Mass spectrometry/ICP-MS

Published in the topical collection *Single Cell Analysis* with guest editors Petra Dittrich and Norbert Jakubowski.

L. Mueller (✉) · H. Traub · N. Jakubowski · D. Drescher · J. Kneipp
BAM Federal Institute for Materials Research and Testing, 12200 Berlin, Germany
e-mail: larissa.mueller@bam.de

D. Drescher · J. Kneipp
Department of Chemistry, Humboldt-Universität zu Berlin, Brook-Taylor-Str. 2, 12489 Berlin, Germany

V. I. Baranov
DVS Sciences Inc., Markham, ON L3R 6E7, Canada

Introduction

In recent years, a growing interest in single-cell analysis can be recognized and numerous analytical methods have been developed or improved to allow the analysis of individual cells and their cellular compartments. The aim of most of these studies is related to identification and quantification of all or at least many components in cellular systems with spatial and/or temporal resolution. Reams of new developments of different methods have been applied so far, such as fluorescence microscopy, mass spectrometry, mass spectrometry imaging, electrochemistry imaging, and lab-on-chip devices. An overview of these methods and more is presented in different review articles [1–6]. The reason for this research interest is that the common lysate-based assays provide only integrated information, but not all cells respond alike. If we want to understand the "whole story" of rare cell populations, the biology of individual cells needs to be studied.

This article is focused on highlighting the most recent trends and applications in which ICP-MS (partly ICP optical emission spectrometry ICP-OES) is applied for single-cell analysis using metal atoms that are intrinsically present in cells, taken up by cells (for instance uptake of engineered metallic nanoparticles by cells), or which are bound to a cell or cell component. Using inductively coupled plasma mass spectrometry (ICP-MS) for single-cell analysis is a very new and fast growing research field, and the applications are not well established and still far from being routine.

ICP-MS is a mass spectrometric multi-element method based on counting the number of atoms in a sample. It provides easy sample preparation, multi-elemental detection combined with high sensitivity (ng L^{-1} range), and large dynamic range (up to nine orders of magnitude), and can often be calibrated by simple standards, thus offering the advantage of providing quantitative information. Additionally, isotope ratio measurements are accessible and isotope-labeled

experiments are possible. Owing to its outstanding sensitivity, it is more and more applied for detection of elements and, in particular, metal atoms in life science applications [7]. Presently, single-cell analysis is becoming a new research direction in which elements and, in particular, metal atoms present naturally or intentionally bound to a single-cell component are detected at ultra-trace levels directly or indirectly by ICP-MS. The challenges using ICP-MS in combination with pneumatic nebulizers for single-cell analysis involve the integration time (limited by the instrument) and the sampling rate needed for adequate detection of real single-cell events.

In the past, biological cells have been investigated as a digestion of a cell suspension or pellet containing typically 10^6 cells [8, 9]. By averaging over a huge ensemble of cells, all individual variations are lost and no information about the distribution within a cell is available. To overcome these limitations, different methods for the elemental imaging based on microscopic, mass spectrometric, and spectroscopic techniques have been developed in recent years and are subject of several reviews [10–15].

The novel capabilities of laser ablation as a sample introduction technique in ICP-MS are applied more and more for advanced imaging mass spectrometry for direct analysis of solid and soft materials. LA-ICP-MS provides spatially resolved information on element distribution (qualitative and quantitative) in thin sections of biological samples, for instance of brain tissue, to study neurodegenerative diseases or tumour growth [16, 17]. By rastering the sample with a laser, a one- or two-dimensional image can be reconstructed that shows the relative intensities of the respective elements. This technique is thus most often applied for qualitative imaging of biological samples (bio-imaging) at a resolution between 500 and 20 μm [18]. Though the development of suitable calibration standards and internal standards for standardization and accuracy are still under investigation [19], Internal Standards for laser ablation have to correct differences in the LA process caused for example by drift effect or variations in the sample properties. Therefore, matrix matched in-house standards are often used. Various normalization approaches and quantification strategies are described in detail in the reviews from Konz et al. [16] and Hare et al. [19].

Reducing the laser spot size is inherently related to a reduction in sensitivity, due to the fact that the volume/area and, thus, the number of atoms in this volume (area) is tremendously reduced. Thus, a compromise between sensitivity and spot size is usually driven by the application, and this was the reason why imaging with single-cell resolution has not been investigated frequently. In a recent study of Wu et al. [20], a laser micro-dissection system was coupled to an ICP-MS and used for detection of hetero-elements in brain tissue at laser spot sizes ranging from 30 down to 4 μm. Although single-cell detection was not demonstrated, this example clearly shows that some elements can be detected already in biological systems at natural levels even with smallest laser spot sizes.

While the use of LA-ICP-MS for single-cell imaging is just at its beginning, other technologies like X-ray fluorescence (SXRF) microscopy and secondary ion mass spectrometry (SIMS) showed already that the imaging of biological trace metals at nm scale is possible [14]. The methods (including LA-ICP-MS) differ amongst others in field of view, spatial resolution, mass range, detection limit, dynamic range, and the number of simultaneous elements. Depending on these parameters and the sample characteristics, the most suitable technique has to be chosen. A detailed comparison is not part of this review, but is given in Reference [14].

Measuring metal atoms at the cellular level might help to better understand fundamental biological functions of metallo-proteins, in particular metallo-enzymes or even metallo-metabolites, and might give the basis to differentiate between healthy or diseased cells. Although the metal content does not completely reflect the biochemistry of a cell, a change in the metal composition can be used as a first hint and motivation to look deeper into the biological molecular processes involved. For the latter purpose, ICP-MS techniques based on metal tagged probes (e.g., antibodies, proteins, amino acids) can be used for indirect detection of the biomolecule of interest.

Label free analysis by ICP-OES/MS

Liquid ICP-OES/MS

Pneumatic nebulization of cell slurries

Nomizu et al. [21] used a liquid sample introduction system in combination with ICP-OES for the determination of calcium in individual mammalian cells. The diluted cell suspension was sprayed by a concentric nebulizer and the droplets (with one cell or without) were dried in a heated drying chamber and introduced into the ICP. However, the introduction efficiency of dried cells into the ICP was less than 0.1 %. For calibration, a calcium acetate aerosol was generated by a vibrating orifice mono-disperse aerosol generator. The Ca content of three different mammalian cell samples (cell diameter 10 – 20 μm) from cell cultures was determined between 0.057 and 0.27 pg per cell with a detection limit in the range of 0.01 pg per cell. [21]. Applications to the determination of other elements like Na, K, or Mg in individual cells were limited because the sensitivity of the ICP-OES was too low. Utilization of an ICP-MS may overcome this problem.

A full multi-element analysis of single cells was first performed by Haraguchi's team, who investigated the ionome of single or multiple salmon egg cells and coined the term

"metallomics" [22, 23]. They determined 78 stable isotopes of different elements and detected 74 of them in 3 salmon egg cells by ICP-AES and ICP-MS after microwave digestion [22]. Many essential trace elements showed extremely high bioaccumulation factors (compared with sea water) ranging from more than 1.0×10^4 for Cu, Zn, Co, Mn, P, Se, and Hg to 5.0×10^5 for Fe. Bearing in mind that salmon eggs have a diameter of a few mm, the real challenge starts with normal biological cells with dimensions at the μm scale.

The direct label free analysis of much smaller single cells by ICP-MS has been first reported by Houk's group [24]. They measured the signal of uranium incorporated intrinsically in *Bacillus subtilis* using a micro-concentric nebulizer (about 10^8 cells per mL). The ICP-SFMS was operated with an integration time of 4 ms, which is the fastest sampling possible with the magnetic sector field instrument used (Element 1). The observed U^+ spikes were related to intact bacteria, as such spikes were only detected when bacteria are present in the sample solution. The spikes cannot be clearly attributed to a single cell embedded in a droplet. They also showed that by sonification, the bacteria increased the U^+ response by 30 %, which was interpreted as a hint of severe matrix effects because cells behave more like a micro-particle rather than a droplet.

Recently, Ho and Chan used a conventional pneumatic V-groove nebulizer and analyzed algae covering a range of cell diameters from 1.3 to 5.3 μm [25]. In their work, they used an integration time of their quadrupole-based ICP-MS of 10 ms in time-resolved analysis mode. They mainly measured Mg in the cells, but detected a few cells containing Mn and Cu as well. With their setup, they additionally studied metal adsorption of Cr on the cell surface.

Tsang et al. [26] monitored the metal content in *Helicobacter pylori*. A magnesium content of about 2.9×10^7 atoms/cell for the wild-type *Helicobacter pylori* was determined using MgO nanoparticles as calibration reference. The methodology was validated using a batch type method and found to be 2.52×10^7 Mg atoms/cell, which is in good agreement with the single-cell measurement. The application of the developed method was demonstrated by tracking the uptake of a Bi anti-ulcer drug. Bacteria treated with a Bi-based drug deposited nearly 1.0×10^6 Bi atoms/cell, whereas the uptake process took about 3 h to reach the half-maximum. The protective effect of ferric citrate against bismuth complex accumulation by *Helicobacter pylori* was also investigated.

Trace elemental analysis of single yeast cells with time-resolved ICP-MS using a high efficiency cell introduction system was carried out by Groombridge et al. [27]. The sample introduction system consists of a high performance concentric nebulizer and a custom-made 15 mL on-axis spray chamber utilizing a sheath gas flow. This system was used for the multi-element analysis of yeast cells (*Saccharomyces cerevisiae*) with a diameter of about 4 μm. Cell adsorption to tubing, nebulizer, and injector was reduced by adding a NaCl solution to the cell suspension. With the optimized system, a cell transport efficiency of 75.0 %±4.7 % was obtained. Time-resolved analysis using an ICP quadrupole mass spectrometer at its lowest integration time of 10 ms was used. Thereby signals corresponding to separated cell events were detected for Mg, P, Ca, Mn, Fe, Cu, and Zn. Additionally, first experiments using ICP time of flight mass spectrometry for single-cell analysis were performed, allowing quasi-simultaneous multi-element detection and making element correlation analysis in yeast cells feasible.

Furthermore, single-cell ICP-MS was successfully applied by Zheng et al. [28] for the determination of quantum dots (QDs) in Raw 264.7 cells (a mouse leukemic monocyte macrophage cell line). The uptake of carboxyl CdSeS QDs (diameter 7 nm) in single cells after exposure was quantified using a Cd standard solution for calibration. The number of QDs per cell was found to be in good agreement with the ICP-MS results after digestion of the cell suspension. Additionally, the uptake kinetics were studied by incubating the cells with QDs for 2 to 12 h.

Injection of cells by use of micro-droplet generation

The drawback of conventional pneumatic nebulizer based methods is the long integration of several ms, as well as the sampling rate. To overcome these limitations, a very fast scan mode of a sectorfield ICP-MS (Element XR) was discussed by Shigeta et al. for measurement of single droplets injected into the plasma by use of a piezo-electric micro-droplet generator (μDG) [29]. Usually, a sample solution is continuously introduced into the plasma by pneumatic nebulization, with typical integration time in the range of a few ms or higher, which is much too long in order to measure the fast transient signals generated by injection of a single droplet of about 500 μs, for which an integration time as low as 100 μs is essential.

In a first application, the micro-droplet generator was applied by Shigeta et al. as a sample introduction system for the injection of single cells directly into an ICP-SFMS to measure metal atoms in individual cells time-resolved [30]. For this purpose, cells had been embedded into single droplets generated by the μDG. Selenized yeast cells with a diameter of roughly 6 μm have been used as a model system for these investigations. A fixed droplet generation rate of 50 Hz produced equidistant signals in time of each droplet event and was advantageous for separating the contribution of background and blank from the analytical signal of the cell.

This is shown by means of Fig. 1, in which a time-resolved measurement of the $^{63}Cu^+$ ion intensity burst generated from a single-cell event only is presented. Cu is just an example for a typical essential element in the cell. A few hundred counts were detected for $^{63}Cu^+$ with a total amount of only 300

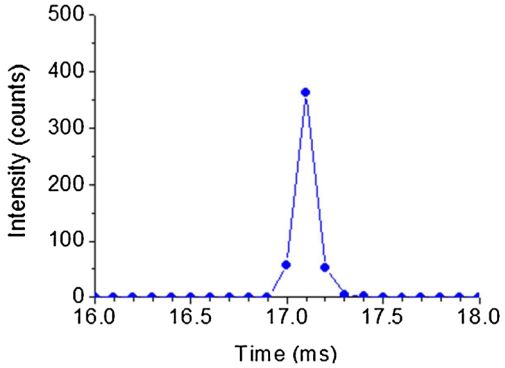

Fig. 1 Time-resolved $^{63}Cu^{+}$ signal intensities of a single yeast cell embedded in a single droplet generated by the micro droplet generator system. Parameters: 0.05 cell/drop; sample integration time: 0.1 ms; counting mode. With permission from J Anal Atom Spectrom

attogram in the cell, from which the LOD can be estimated at low attogram level because the noise level is rather low. The signal of just a single cell is measured time-resolved with an integration time 100 μs per increment, which is equivalent to 4.0×10^{6} cps, and coming close to the saturation of the ion counting mode of the detector. Therefore, most elements in this investigation had to be measured in the analog mode, demonstrating that presently ICP-MS has much more sensitivity left to even detect less abundant elements.

Open vessel digestion and a multi-element analysis were performed with washed yeast cells, and absolute amounts per single cell were determined for Na (0.91 fg), Mg (9.4 fg), Fe (5.9 fg), Cu (0.54 fg), Zn (1.2 fg), and Se (72 fg). Signal intensities from single cells have been measured for the elements Cu, Zn, and Se, and histograms were calculated for about 1000 cell events. The mean elemental sensitivities measured here range from 0.7 counts per ag (Se) to 10 counts per ag (Zn) with RSDs from 49 % (Zn) to 69 % (Se) for about 1000 cell events. It is not yet resolved definitively if this RSD expresses the individual variability of cells or if the cells have an impact on the droplet formation.

A novel microfluidic system for droplet generation and direct injection into the ICP-MS was recently presented by Verboket et al. [31]. The core component of the system is based on liquid assisted droplet ejection (LADE) chip, which is made entirely of poly(dimethylsiloxane) (PDMS) and generates droplets at about 50 μm diameter, in which single cells can be embedded in a highly volatile oil phase. Owing to the large size of the droplets, a CETAC U 6000 membrane desolvator was used to reduce the droplet size before injection into the plasma. Intensities for $^{56}Fe^{+}$ of about 400 cps have been measured representing 5×10^{8} atoms in a blood cell, a value which agrees well with the bulk concentration measured.

Both examples demonstrate that dedicated sample introduction systems look very promising for single-cell analysis by ICP-MS.

Additional ICP-OES/MS based techniques for single-cell analysis

Another way is the direct vaporization of small volumes (sub-nL) or single cells in combination with ICP-OES/MS. The group of Hu [32, 33] used electrothermal vaporization ICP-MS without and with chip-based micro-extraction for trace element determination in different cell lines. Recently, they were able to determine Bi, Cd, Cu, Hg, Pb, and Zn in a small number of cells (5.0×10^{3} to 3.0×10^{5} HepG2 or Jurkat T cells), but not at single-cell level.

Badiei et al. [34] were able to determine the Ca content of individual cells by rhenium-cup in-torch vaporization (ITV) sample introduction coupled to ICP-OES [35]. *Paramecium bursaria* cells with an average size of about 150 μm were used in this study. An isolated cell plus water (volume about 0.1 nL) are pipetted into a rhenium-cup and inserted into a vaporization chamber by using a special sample holder. Electrical power is applied to the cup to dry and vaporize the sample. The vapor is then inserted into the central channel of the ICP. Diluted Ca solutions were used for calibration. Special care was taken to avoid Ca contamination of the sample and losses by Ca diffusion out of the cells. The presented approach enables to determine the cell-to-cell variability of the Ca content of *Paramecium* species.

Detection of nanoparticles or elements in single cells by LA-ICP-MS

Considering the great influence that nanostructures can exert on biological matter, including single cells that are currently standard models used to understand nano-bio-interactions, the emergence of nano-toxicology as its own extensive field of research appears highly plausible. To elucidate how the physico-chemical properties of a nanomaterial are in fact connected with the local distribution and the number of nanoparticles, the uptake of a nanomaterial has to be quantified, and the intracellular fate, including major sites of accumulation, has to be determined. To obtain information on nanoparticle localization inside the cellular ultrastructure at very high resolution, electron and X-ray microscopic methods are often used [36–38]. Since the sample preparation (e.g., staining, sectioning) and measurement procedure are extensive and time-consuming, these ultra-structural methods are rarely applied for particle quantification. There are only very few methods that can attain spatial localization of inorganic nano-materials inside a cell and provide quantitative information about them in situ. Recently, the potential of LA-ICP-MS for the investigation of nanoparticle uptake and distribution by micro-mapping in single eukaryotic cells was demonstrated by Drescher et al. [39, 40]. Highly resolved images visualizing

the relative amount and two-dimensional distribution of silver and gold nanoparticles were obtained by use of a special "differential scanning" mode with a commercial LA system [NWR213; ESI (ElectroScientific Industries, Bozeman, Montana, USA)]. For this purpose, the laser energy was optimized to ablate the sample completely with every laser shot without affecting neighboring regions. Scan speed and ablation frequency were adapted to the laser spot size of 4 or 8 μm so that the laser spots are widely overlapping and the signal of the sample is generated only by the new incremental area ablated (Fig. 2). Thus, the lateral resolution in scan direction is much better than the laser spot diameter. However, the lateral resolution also depends on the wash-out time of the laser ablation chamber and the data acquisition frequency of the mass spectrometer. Very recently, the spatial resolution was significantly improved by combining a LA system with a low-dispersion LA chamber and an ICP time-of-flight mass spectrometer (TOF-MS), but this will be discussed in more detail in a later section [41, 42].

By spatially resolved bio-imaging Drescher et al. were able to localize silver and gold nanoparticles in individual fibroblast cells (cell line 3 T3) upon different uptake experiments [39]. For the cell experiments, fibroblast cells were grown as monolayer on sterile coverslips and incubated with different metallic nanoparticles under standard cell culture conditions. Figure 3a displays an example of a data set obtained with cells that were incubated with gold nanoparticles. The comparison with light micrographs and similar samples that were studied by electron microscopy and cryo nano-scale X-ray tomography [40] showed that the distribution of the metallic nanoparticles with respect to cellular substructures is well reflected by the LA-ICP-MS maps, and the nanoparticles are found to accumulate in the perinuclear region (Fig. 3a). In the case of silver nanoparticles, it was shown by LA-ICP-MS micro-mapping that increasing particle concentration in the culture medium and incubation time leads to an increase of the $^{107}Ag^{+}$ intensity inside the cells, which can be directly correlated with an increasing number of nanoparticles [39]. To obtain the nanoparticle concentration per single cell, a quantification method based on matrix-matched calibration using nitrocellulose membrane doped with silver or gold particle suspensions was applied (Fig. 3b). The studies provide evidence of a high amount of silver nanoparticles (up to about 5.7×10^4 per cell)

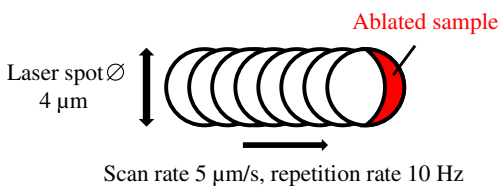

Fig. 2 Schematic presentation to illustrate differential scanning applied for the localization of nanoparticles in single cells

in the cellular matrix (Fig. 3c), which is in accordance with ICP-MS results that were obtained by other groups after digestion of cell suspensions [43].

Recently, LA-ICP-MS was also used to study the interaction of silica nanoparticles with eukaryotic cells using silica nanoparticles with a gold or silver core, termed BrightSilica [40]. Since the physico-chemical properties of the nanomaterial, e.g., size and surface modification, determine the mechanism and efficiency of cellular uptake, silica coating of a metal nanoparticle can be expected to result in differences in the quantitative particle distribution and also in the cytotoxic behavior, and the BrightSilica particles would in that sense mimic pure silica nanoparticles. Owing to the low sensitivity and high background signal, the silica itself would not be applicable for high-resolution LA-ICP-MS imaging. The concept of using an identical-size metal core for detection and quantification provided the possibility of comparing cellular uptake of the coated silica-like nanoparticles with different silica thickness, and also with uncoated silver nanoparticles. By comparison of the 2D LA-ICP-MS intensity maps (compare Fig. 4b and e) one notices significant variation in the total number of particles internalized by the 3 T3 cells upon incubation, depending on the thickness of the silica shell [thin (Fig. 4a) and thick silica shell (Fig. 4d)]. As the same core size was used, the different shell thickness results in different particle diameter, and the larger nanoparticles (diameter of ~120 nm) are taken up with lower efficiency than the smaller ones with thin shells (diameter of ~60 nm) [40]. Furthermore, the examples showed that LA-ICP-MS is a valuable method for assessing cell-to-cell variability regarding size, morphology, and uptake behavior in the single-cell analysis.

In the context of uptake investigations, the results of LA-ICP-MS analysis are combined with ultra-structural information from X-ray tomography and in situ molecular information from surface-enhanced Raman scattering (SERS). For the example of the silica-coated nanoparticles [40], the plasmonic metal core, which serves as SERS substrate providing a local optical field [44], can be used to characterize the molecules interacting with the silica surface. SERS chemical images of the intensity distribution were obtained based on the Raman signal at 665 cm^{-1} (Fig. 4c), assigned to the C–S stretching vibration of cysteine in peptides and proteins and at 1582 cm^{-1} (Fig. 4f), which corresponds to the C–C stretching vibration of an encapsulated reporter molecule (*para*-aminothiophenol) in the nanoparticles with the thick silica layer. As can be seen in Fig. 4c, f, the perinuclear regions comprise high-intensity pixels, indicating that most nanoparticles accumulate around the nucleus, in accord with the LA-ICP-MS data. The combination of LA-ICP-MS micro-mapping with Raman microspectroscopy illustrates that chemical information from both the nanoparticle and the biological system is needed to obtain insights into the particle/cell interactions, and into the distribution and quantity of nanoparticles in single cells, which is

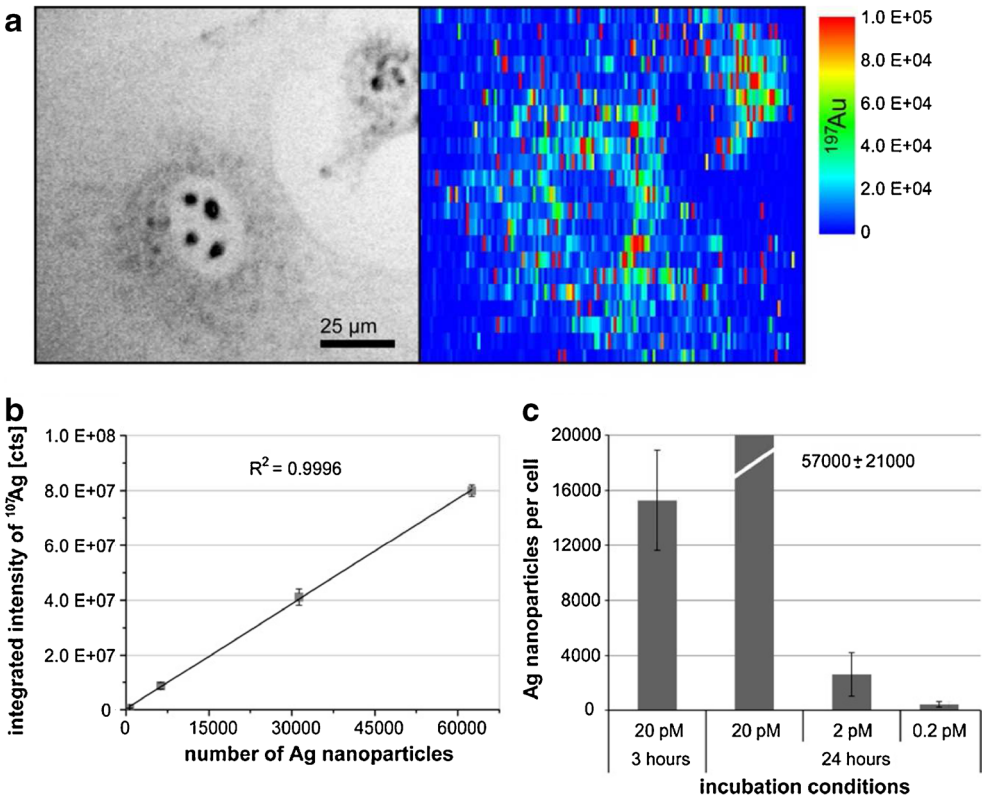

Fig. 3 (**a**) LA-ICP-MS image of the $^{197}Au^{+}$ intensity distribution (in cps) inside a single fibroblast cell after incubation with gold nanoparticles (100 pM, 3 h) and the corresponding bright field image. Parameters: laser spot size 4 µm, scan speed 5 µm/s, repetition rate 10 Hz, fluence 0.8 J cm^{-2}. Based on matrix-matched calibration data (**b**) the number of silver nanoparticles is quantified for individual cells (**c**). Parameters: laser spot size 8 µm, scan speed 8 µm/s, repetition rate 5 Hz, fluence 1.5 J cm^{-2}. Adapted with permission from Drescher et al. [39]

important for understanding their intracellular processing and cytotoxic behavior. Besides this combination, there are also other mass spectrometric approaches to investigate the intracellular distribution of nanoparticles and the chemical composition of the cells at high lateral resolution. For example, time-of-flight secondary ion mass spectrometry (TOF-

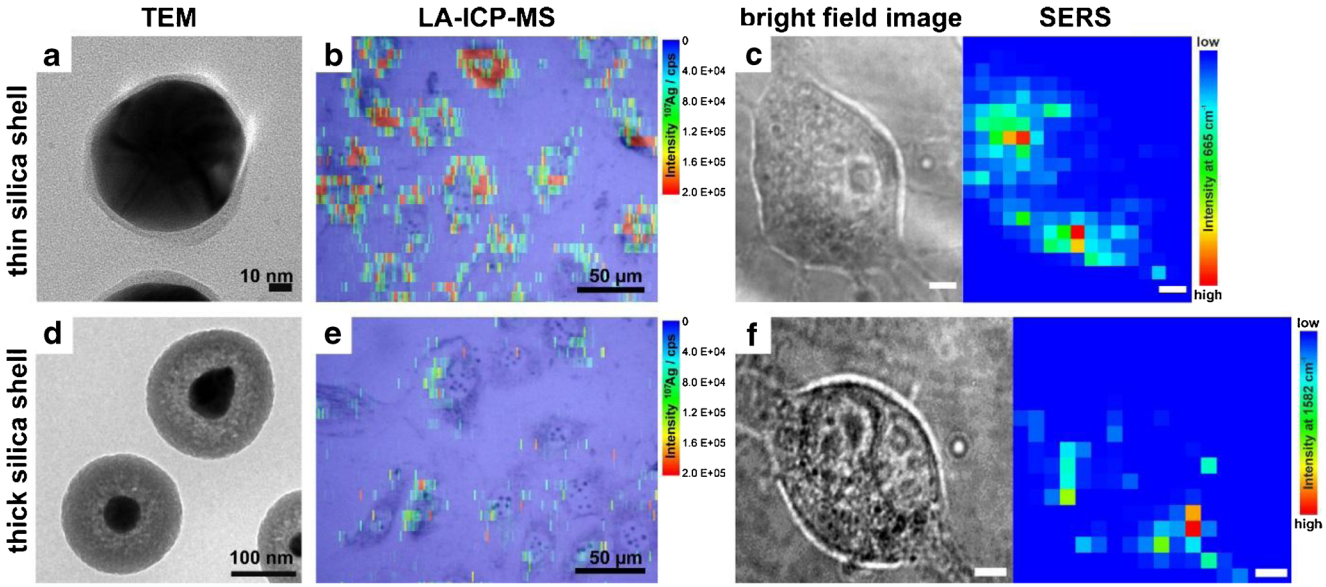

Fig. 4 In situ characterization of particle/cell interaction using silica-coated silver nanoparticles. Transmission electron micrographs (TEM) reveal thin (**a**) and thick silica shell (**d**) around silver nanoparticles. (**b**) and (**e**) Bright field micrographs superimposed with LA-ICP-MS images of $^{107}Ag^{+}$ intensity distribution of fixed fibroblast cells after exposure to core-shell nanoparticles. Parameters: laser spot size 8 µm, scan speed 8 µm/s, repetition rate 5 Hz, fluence 0.6 J cm^{-2}. (**c**) and (**f**) SERS chemical maps and the corresponding bright field images of 3 T3 fibroblast cells incubated with silica-coated silver nanoparticles (scale bars represent 4 µm). The intensity distribution of the SERS signal at 665 cm^{-1} [ν(C-S) of cysteine] and at 1582 cm^{-1} [ν(C-C) of *para*-aminothiophenol] are displayed. Excitation wavelength: 785 nm, accumulation time: 1 s, intensity: 1.9×10^{5} W cm^{-2}. Adapted with permission from Drescher et al. [38]

SIMS) and laser secondary neutral mass spectrometry (Laser-SNMS) have been utilized for the localization of nanoparticles inside cells with resolutions down to 100 nm [45, 46].

Although in some cases only very few nanoparticles, consisting of millions of gold or silver atoms, are present per single spot, the sensitivity of the LA-ICP-MS allows the investigation of even less amounts of metal atoms. Examples of this are (metallo-) proteins or the tagging of antibodies by metal atoms, which are used for signal amplification. This issue will be further discussed in another chapter.

A different type of signal amplification will be discussed in the next example. Here bio-enrichment of metals by living cells is used as the prerequisite for LA-ICP-MS detection of single cells. Managh et al. report the first LA-ICP-MS application to perform single-cell detection of T-cell populations relevant to cellular immunotherapy [47]. In this example, the cell diameter (about 10 μm) was much smaller than the laser spot diameter (25 μm), so that in each laser shot a single cell was completely ablated. To ensure single cell targeting, labeled cells were plated onto slides in adequate cell density, and cells closer than 25 μm apart were not considered. Purified human $CD4^+$ T-cells were incubated with commercially available Gd-based magnetic resonance imaging (MRI) contrast agents (Omniscan and Dotarem) in different concentrations and for different incubation times. In the chelated form, these substances are not toxic, highly water soluble and bioavailable and these features enabled passive loading of up to 10^8 Gd atoms per single cell under optimum conditions. LA-ICP-MS single-cell analysis demonstrated that the cells retained a sufficient marker to remain detectable for up to 10 d post-incubation both in vitro and in vivo in an immunodeficient mouse model. This experiment can be used for studying the uptake of contrast agents by cells in pharmacokinetic studies in the future.

ICP-MS analysis after tagging

Biomolecules can be detected directly by ICP-MS in cells if they contain a detectable hetero-element (as described in a chapter above), or if artificial tags or labels are attached to the biomolecule of interest. Alternatively, the target protein can be identified indirectly by use of a substance specific antibody in an immunoassay. In the following chapter, first selected tagging strategies for antibodies having regard to single-cell analysis by ICP-MS will be discussed, before selected applications are presented.

Indirect detection of biomarkers in or on cells by use of metal tagged antibodies

Metal tags are often used for the modification of antibodies, which recognize the target protein (antigen) specifically via the key-lock-principle (immune reaction). In this way, the ICP-MS detection of the element tag attached to the antibody allows the indirect identification—and in case of imaging technologies the localization—of a specific target protein in a complex sample.

In recent years, bifunctional ligands were established as tagging reagent [48] containing two parts, a macrocycle like 1,4,7,10-tetraazacyclododecane-1,4,7,10-tetraacetic acid (DOTA) or diethylenetriaminepentaacetic acid (DTPA), and a reactive group which connects covalently to the antibody. The DOTA macrocycle or the linear chain DTPA can be loaded by different metals such as lanthanides. The lanthanide elements are preferred because of their similar chemistry and low natural background in biological samples. The 13 lanthanide elements provide at least 37 isotopes that are non-redundantly unique masses allowing the design of highly multiplexing/multi-parametric cell assays. For more details, see the reviews related to the chemistry and history of metal tagging [18, 48].

Most applications deal with tags containing only one detectable element. Depending on the linking chemistry, an average between 1 and 4 detectable atoms per antibody are introduced [49]. In the context of single-cell immunoassays and very low abundant analytes (ag or zg range) these tagging degrees are not sufficient because the sensitivity of the ICP-MS (signal per unit concentration) reaches its limit.

The instrumental reason for this is the low ion transmission of the ICP-MS instrumentation (1 of 10^4 ions are detected in case of ICP-TOF-MS). Theoretically, a minimum of 1.0×10^4 metal atoms must be present on or in a cell before a signal is detected [50]. This is even more critical in the context of single-cell imaging by LA-ICP-MS because in this case the cell is ablated stepwise and introduced partially (dependent on the spot size of the laser) into the ICP-MS.

To compensate this instrumental disadvantage new polymer tags were developed by Lou et al.[51] for cell assays analyzed by ICP-TOF-MS specially designed for this application. The polymer contains various binding sites for DOTA, which results in up to 30 metal atoms per tag. A maleimide group at one end of the polymer chain is used for coupling to free thiol groups generated by partial reduction of the disulfide bridges of the antibody. A number of 2 to 4 polymer tags per antibody are postulated by the researchers, which could be equated with 60 to 120 detectable atoms per antibody, resulting a sufficient intensity enhancement for ICP-MS analysis even in a single-cell assay [52].

As described before, often a maleimide residue is used as a reactive group binding to the antibody because of high tagging degrees and excellent sensitivity in ICP-MS based immunoassays [49, 51, 53, 54]. The drawback of the maleimide tagging chemistry is the necessity of partial reduction of the antibody to generate free sulfhydryl groups for binding. Thus, each new antibody needs to be validated after tagging to proof

its specificity for the target antigen. Additionally, the formation of different antibody fragments with various tagging degrees complicates the development of quantification concepts, for which the knowledge of an exact tagging degree and the ratio between number of antigens to antibody is a prerequisite [55]. Thus, from an analytical point of view, quantitative immunoassays would be highly desirable and ICP-MS would be an ideal detector for this purpose, but presently more investigations are needed to validate the calibration of these assays.

Mass cytometry

The state-of-the-art for characterizing proteins of many cells individually is flow cytometry. A cell sample is treated with fluorescence probes (e.g., antibodies), and the cell suspension is formed to a liquid stream, which allows the aligned cells to pass a light beam for fluorescence sensing. Since the technique is limited by spectral overlap, fluorescence dye quenching and auto-fluorescence of the sample multiple parameters should be analyzed simultaneously. A novel technique for real time analysis of multi-parameter assays of single cells at high throughput was developed by Tanner and colleagues [52, 56]. The antibodies have been modified with metal tags as described elsewhere instead of fluorophores conventionally employed in polychromatic flow cytometry.

The mass cytometer (Fig. 5), which employs a fast ICP-TOF-MS, was introduced to the market as CyTOF by DVS Sciences Inc., Markham, Canada. It is a novel adaptation of atomic mass spectrometry to address the challenges of polychromatic flow cytometry. In the spray chamber, the turbulent gas flow containing droplets with embedded cells is dried (all water droplets without cells are vaporized) and converted into a laminar flow. Stochastically spaced cells in the laminar flow are then delivered concentrically to the plasma core. A consensus model considers a cell in plasma generating an ion cloud, which rapidly diffuses on its way downstream of the plasma core. The ion cloud from an individual particle or cell is large enough to produce a transient signal of ~280 μs of a pseudo-Gaussian shape. The resulting ion cloud is much larger than the parent cell and is diffusion limited. After full thermolytic decomposition, atomized and ionized cells transform into approximately spherical ion clouds and propagate through the atmosphere–vacuum interface, ion beam forming optics, time-of-flight mass analyzer, and finally, are registered by the detector and data acquisition system as a transient event: ion intensity versus time.

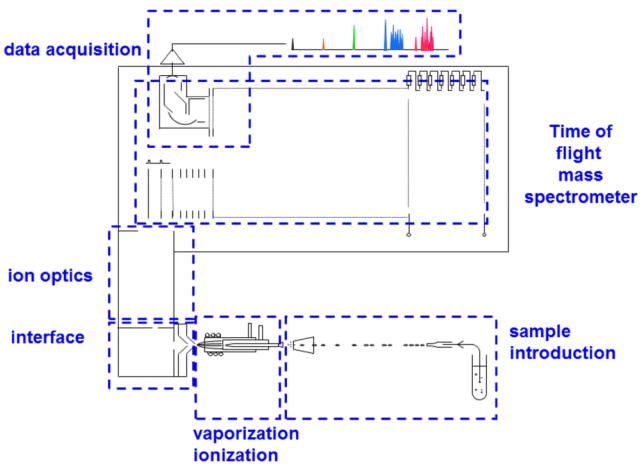

Fig. 5 Schematic setup of a mass cytometer

The stochastic sample introduction leads to possible overlap of the ion clouds limiting the maximum rate of cell introduction to ~1000 per s. It is shown that a metal-containing DNA intercalator is capable of revealing important information about the transient event in mass cytometry, allowing it to be applied for the recognition of single-cell events, cell fragments, and to qualify the acquired data [57]. Spectra are recorded at 13 μs intervals. Between cell events, the spectra are largely blank (reflecting only the metal content of the solution between cells, which may contain metals associated with antibodies that have dislodged from the cells and, therefore, does not provide a suitable "negative" background; see also Fig. 6). When an ion cloud arrives at the detector, a series of some 20 spectra reflects the Gaussian-like transient and contains all of the metal ions associated within the cell, including those metal isotopes that were intentionally attached as probes (of antibodies, DNA, and viability indicators).

The analysis is complicated by very fast data stream and is implemented on-the-fly (directly during the acquisition process), in-line (immediately after the acquisition stream before the next sample), or off-line in post-processing mode. For example, on-the-fly visual confirmation provides a real time display of the first 3 ms of data acquired each s, as an indicator of satisfactory analytical conditions. An example is provided in Fig. 6, showing a screen capture during the analysis of a human peripheral-blood mononuclear cell (PBMc) sample stained with 27 metal-tagged antibodies. The display indicates a pixel each time an ion signal is recorded, and shows the masses along the X-axis and the sequential spectra along the vertical axis. It is clear that the raw data clusters in two dimensions are aligned, indicating a complex and unique ion structure of every ion cloud.

Multi-parametric transient data streams generally represent a substantial challenge for data acquisition systems and subsequent analysis. In the case of mass cytometry, such software allows interrogation of the data through a set of orthogonal bivariate dot plots that display the correlation of two parameters for each cell. A typical four-parameter (n=4) experiment can be represented by six such bivariate plots [0.5 n (n - 1)]. A 32-parameter mass cytometry data set is represented by 496 bivariate plots, each of which can be gated and expanded in

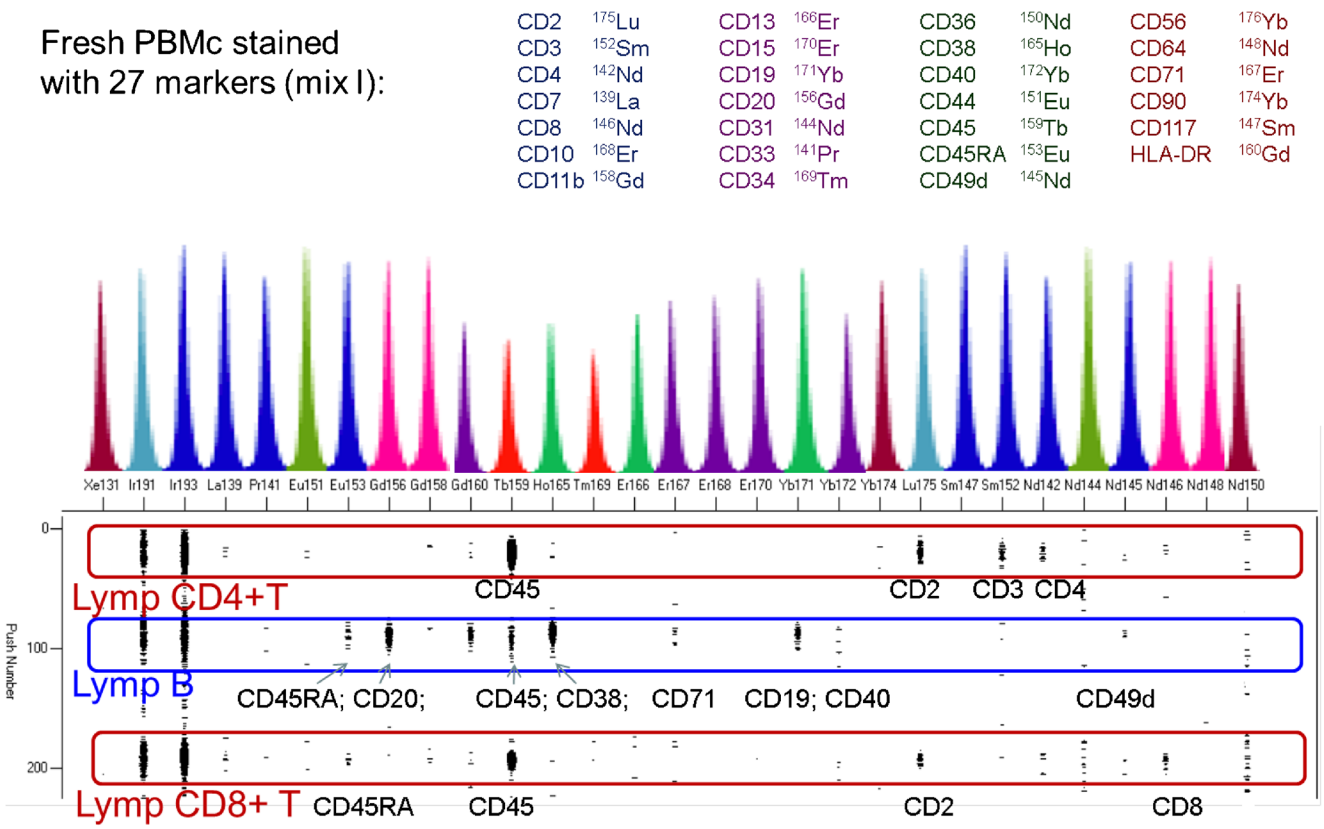

Fig. 6 A screen capture of raw digitized data for slurry nebulization of a human PBMc sample stained with 27 metal-tagged antibodies and with Ir containing DNA-intercalator. The concomitance of the metal tag and intercalator signals identify a single-cell event

the remaining 30 dimensions. The complexity of such data sets arises and it is nearly impossible to identify an overall trend, and especially small changes in selected cell subpopulations. The application of bioinformatics for multi-parametric cytometry data sets is needed. Bendall et al. generated an immuno-phenotyping tree with the SPADE algorithm (www.cytobank.org), which groups cells of identical phenotype into clusters, connected to each other based on similarity in a tree structure [58, 59]. Thirty-one markers were analyzed by CyTOF technology characterizing the functional response of the entire human hematopoietic system to immune modulators and small molecule drug inhibitors in human bone marrow samples. This analysis greatly increases the understanding of cell types and their relationship to each other within normal bone marrow, and enables presentation of the bone marrow as a continuum of phenotypes.

The application of an elemental barcode by Bodenmiller et al. even increases the high-throughput cell screening by mass cytometry. Seven maleimide-DOTA loaded with lanthanide isotopes were used to generate 128 combinations, enough to barcode each sample in a 96-well plate. The cells in each well were labeled with a unique isotope composition, and then they were pooled into a single tube for the immunoassay with metal-labeled antibodies. For each of 27 inhibitors, 14 phosphorylation sites were analyzed in 14 PBMC types at 96 conditions, resulting in 18,816 quantified phosphorylation levels from each multiplexed sample [60].

For more details about data handling of massively multi-parametric single-cell assays analyzed by CyTOF technology, please see review [61]. The applications of mass cytometry span a whole range of fundamental research, clinical research, and pharmaceutical areas. The latest applications are summarized in Table 1. For more information on CyTOF developments, the reviews of Björnson et al. [77] and Bendall et al. [50] can be recommended for further reading.

Imaging of cells by element tags and LA-ICP-MS

Elemental cell staining

In the previous chapters, the influence of contrast agents and nanoparticles on cellular processes investigated by LA-ICP-MS have been summarized. In the following, the staining of cells and cellular biomolecules for LA-ICP-MS imaging of single cells will be discussed. The samples are directly treated with the label or tag substance (e.g., iodine, hematoxylin and eosin stain, bifunctional ligands) and often abundant molecule groups like selected amino acids (e.g., tyrosine, cysteine) or glycol residues are modified. These lead to a "more general" derivatization of proteins containing the molecule of interest,

Table 1 Summary of applications from mass cytometry

Research	
Cell population characterization; cell viability; cell cycle analysis	[62, 63]
Protein interaction, protein signalling pathways	[58, 64]
Imaging (see also chapter on Imaging of cells by element tags and LA-ICP-MS)	[41, 42]
Pharmaceutical	
Kinase/phosphatase activity	[65]
Stimulation and suppression of phosphorylation or other translational modification	[60]
Drug target validation	[58, 60]
Clinical research	
Diagnostic biomarker panels for accurate diagnosis of disease (cancer, cardiovascular and neurological diseases)	[62, 65–67]
Immunity, vaccine development and testing	[59, 62, 68–73]
Characterization of rare cell populations, and quantitation of those (NK diversity, T cell response)	[74]
Distinction of related disease states (e.g., pathology of leukemia)	[66]
Transplantation and regenerative medicine	[75, 76]

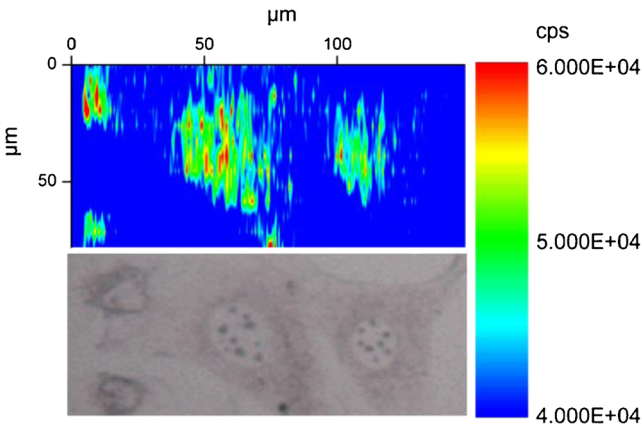

Fig. 7 Lower part: microscopic picture of fixed, iodinated fibroblast cells. Upper part: LA-ICP-MS image of iodine distribution. Laser parameters: spot size 4 µm, scan speed 5 µm s^{-1}, repetition rate 5 Hz, energy 0.7 mJ cm^{-2}, distance in between the line scans 6 µm. With permission from J Anal Atom Spectrom

which results in an artificial visualization of the targets to facilitate the characterization of tissue or cells by LA-ICP-MS imaging. In case of liquid analysis, the cell staining could be used to mark different cell populations with an elemental barcode.

Giesen et al. [78] first showed the iodination of fixed fibroblast cells (cell line 3 T3) by tri-iodide and LA-ICP-MS on a single-cell level. This procedure leads to an electrophilic aromatic substitution of biomolecules, mainly cell proteins, where iodine is found at the ortho-positions of tyrosine and histidine residues [79].

A photograph of fibroblast cells was taken in advance of laser ablation. Surrounded by the cytoplasm, cell nucleus and nucleoli are clearly visible in Fig. 7. Comparison of the photograph with the LA-ICP-MS image exhibits the highest iodine signal within the cell nuclei, and lower intensities in the surrounding cytoplasm even after a very short reaction time of 60 s only. Iodine was detected with high sensitivity at a laser spot size of only 4 µm, which is approximately one-tenth of the size of a fibroblast cell nucleus.

Because iodine shows quite a high instrumental background (4×10^4 cps in Fig. 8), alternative staining and tagging procedures look promising. Here L. Müller shows a whole cell staining using maleimide-DOTA including Tm as central ion (see Fig. 8) as a first example. As mentioned before, the reactive maleimide group connects to free thiol groups such as cysteine. An incubation time of 30 min was sufficient for LA-ICP-MS imaging in the sub-µm range. The single line scans were ablated with a speed of 6 µm s^{-1} and were 8 µm wide. A distance of only 6 µm in between the line centers were selected to generate overlapping ablation spots. Both applications were performed with a commercial LA system (NWR213, ESI) which is limited to a laser spot size of 4 µm. But in combination with a high repetition rate (20 Hz), a pixel resolution smaller than the laser spot diameter can be achieved as described in another chapter above (see also Fig. 2). The resolution achieved in this first experiment permits the detection of even smaller cells. Thus, novel laser ablation chambers are under investigation with significantly reduced aerosol wash-out times [41, 42], but are presently not commercially available. Significant improvements in lateral resolution seem possible with novel laser ablation systems such as excimer lasers, which offer significantly reduced laser spot sizes. Shorter wash-out times (<< 1 s), smaller spot sizes, and increased repetition rates already look technically feasible but under multi-element conditions, the data acquisition times need to be reduced significantly. Although most recent technologies offer integration times as low as µs even for quadrupole devices, this type of application needs at the end novel fast and simultaneous detection technology. This will be discussed in the next chapter. Of course, the metal staining of the whole cell now can be combined with immunoassays or used in conjunction with nanoparticle studies.

Imaging of target proteins in cells by element tagged antibodies

As discussed before, the main limitations for immunoimaging of single cells by LA-ICP-MS are the low ion transmission of ICP-MS instruments and insufficient wash-out times of LA systems. The development of a novel tube cell by Wang et al. with fast wash-out times of 30 ms for high spatial resolution is a first breakthrough in this field [41]. For

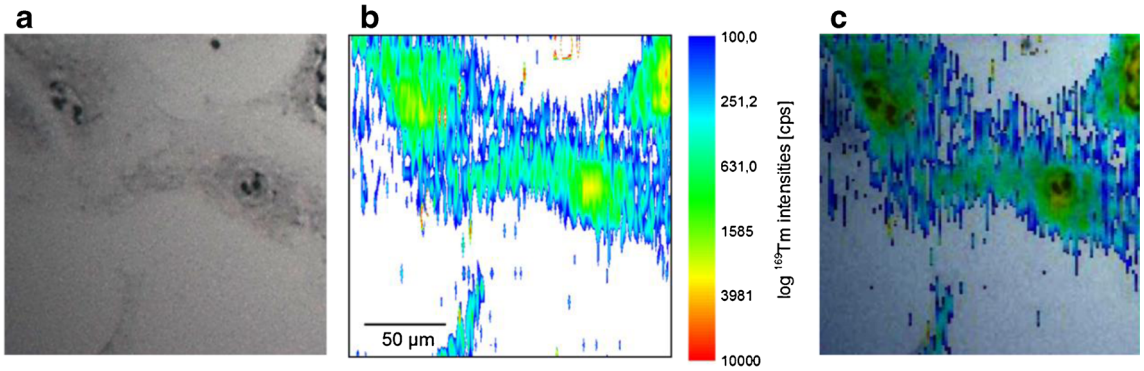

Fig. 8 (**a**) Microscopic picture of fixed and thulium stained 3 T3 fibroblast cells with maleimide-DOTA-Tm. (**b**) LA-ICP-MS intensity profile of thulium distribution. (**c**) Overlay of (**a**) and (**b**). Laser parameters: spot size 8 µm, spot overlay 2 µm, scan speed 6 µm s^{-1}, repetition rate 20 Hz, energy 0,7 mJ cm^{-2}

immuno-imaging of a tissue section, the tube cell was combined with an ArF excimer LA system and coupled to an Element 2 (Thermo Fisher Scientific). A frequency of 20 Hz and a spot size of 1–2 µm were selected to achieve maximum intensity and spatial resolution. The sample was ablated line by line and spot by spot. The dwell time of the MS had to be set to 50 ms to be in accordance with the laser frequency. Under these conditions, only one single isotope could be recorded. A formalin-fixed, paraffin-embedded (FFPE) human epidermal growth factor receptor 2 (HER2)-enriched breast cancer tissue section incubated with a polymer (including Ho) tagged antibody against HER2 was investigated. The resulting image has a pixel size of 1×1 µm and allows a precise analysis of the cell membrane-bounded HER2.

Currently, Giesen and co-workers used the same tube cell in combination with a simultaneous detecting CyTOF for spatially resolved multiplexing immuno-imaging of 32 proteins and their modifications in FFPE breast cancer tissue samples and human mammary epithelial (HMLE) cells [42]. Figure 9 shows an overlay of selected markers at 1 µm resolution. The antibodies were modified with polymer tags containing different lanthanide isotopes. The cell nuclei are clearly identified by histone H3, HER2 is visible in the plasma membrane, and vimentin is shown in the cytoplasm. The results were validated with conventional immunofluorescence microscopy and no significant changes in specificity and performance of the antibodies used for fluorescence and mass cytometry could be observed. Furthermore, it could be shown that even high numbers of metal tagged antibodies did not interfere with each other during the immune reaction. The study reached subcellular resolution for the first time in a multiplex immuno-imaging approach using polymer tagged antibodies and LA-ICP-TOF-MS, but further improvements are still needed. In this study, only selected parts of cancer tissue sections were analyzed with the novel tube cell because an area of 0.5 mm^2 still takes approximately 3.5 h to be ablated with 1 µm laser spot size. Thus, novel commercially available LA systems allowing much higher scanning speeds and sample throughput are urgently needed. Nevertheless, imaging mass cytometry has the potential to significantly advance basic research on tissue heterogeneity and function and might be the next step towards personalized diagnosis and therapies.

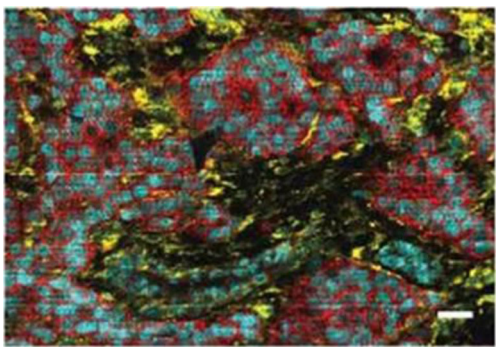

Fig. 9 CyTOF image of luminal HER2+ breast cancer tissue sample. Overlay of HER2 (151Eu, red), H3 (176Yb, cyan), and vimentin (162Dy, yellow). In total, 32 proteins and phosphorylation sites were measured simultaneously at 1-µm resolution. Scale bar, 25 µm. Adapted from Giesen et al. [42]. With permission from Nature Methods

Conclusion and outlook

Single-cell analysis by use of ICP-MS is a new application area in various disciplines (toxicology, medical diagnosis, drug and cancer research, metallomics), which is fast growing and most challenging in terms of sensitivity and multi-element capability.

Depending on the sample introduction system, we can identify two main directions:

– Using pneumatic nebulization for sample introduction into the ICP-MS

  • This type of sample introduction is often used to measure directly cell parameters (especially biomarkers) in

a large number of cells in very short time (1000 or more cell events in 1 s). Therefore, it is particularly suitable for the analysis of huge cell populations, e.g., to determine their hierarchical evolution or the number of cells with pathological modifications. Without being too enthusiastic, for instance metal tagging of antibodies can revolutionize medical diagnosis as well as biochemistry.

– Using laser ablation

  - This type of sample introduction is often used for imaging or immuno-imaging of single cells, although the resolution so far is a limiting factor. The improvements in spatial resolution of the LA systems together with high sensitivity and fast data acquisition of the ICP-MS give reason to expect further insight into element and nanoparticle distribution in (single) cells. An improvement of the lateral resolution of LA-ICPMS to the nanometer scale (down to about 200 nm) is, for example, possible by using the near-field enhancement effect at the tip of a thin silver needle in a laser beam on the sample surface, but such systems are not yet frequently applied [80]. Recently, the ability to image FFPE human breast tumor tissue sections treated with metal tagged antibodies at 200 nm resolution via SIMS has already been demonstrated by Angelo et al. [81]. Nevertheless, resolution at nanometer scale is still a challenge for ICP-MS approaches.
  - Concerning high throughput approaches, single laser shots with high repetition rates are used to ablate each cell by each shot in short time (20 cell events in a second) [47].
  - An open issue for LA-ICP-MS imaging still is the development of quantification concepts and internal standardization. Usually in-house matrix matched standards are used in case of tissue analysis [16]. A first quantification concept in the context of single-cell analysis with LA-ICP-MS was shown by Drescher et al. [39].

All presented studies show that ICP-MS based single-cell analysis offers valuable biologically relevant insights into the element content of individual cell, as well as the uptake of metallodrugs and engineered nanoparticles. But keeping in mind that a cell is a very complex and small machinery with many life functions, which consists of many millions of proteins and their post-translational modifications and, additionally, many billions of metabolites, we get only a snapshot of a very low number of parameters of a highly dynamic and rather complex system. From this point of view (system biology) the information that we can measure is by far not sufficient and, thus, complementing methods are required if multi-parametric function or malfunction of diseased cells have to be investigated. Thus the authors of this article support a new idea of "multimodal spectroscopies," which need to be developed providing more spectral data from atomic and molecular mass spectrometry, synchrotron-based X-ray fluorescence spectroscopy, nano-time-of-flight mass spectrometry, surface enhanced Raman scattering, matrix assisted laser desorption/ionization mass spectrometry, etc. Only the combination of different analytical techniques can expose the secrets of complex systems for a better understanding of the processes and dynamics of biologically or medically relevant cells. Further, we foresee an opportunity in advancing statistical data handling that will allow merging of information from complementary data sets. From a pragmatic point of view, many analytical methods are already fit for purpose at cellular levels, among which ICP-MS is a very promising new tool for single-cell analysis.

Acknowledgement The work of Larissa Müller was funded by the German Research Council (DFG), grant WA 3459/1-1.

References

1. Trouillon R, Passarelli MK, Wang J, Kurczy ME, Ewing AG (2013) Chemical analysis of single cells. Anal Chem 85(2):522–542. doi:10.1021/ac303290s
2. Wang DJ, Bodovitz S (2010) Single cell analysis: the new frontier in 'omics'. Trends Biotechnol 28(6):281–290. doi:10.1016/j.tibtech.2010.03.002
3. Lin YQ, Trouillon R, Safina G, Ewing AG (2011) Chemical analysis of single cells. Anal Chem 83(12):4369–4392. doi:10.1021/Ac2009838
4. Lanni EJ, Rubakhin SS, Sweedler JV (2012) Mass spectrometry imaging and profiling of single cells. J Proteome 75(16):5036–5051. doi:10.1016/j.jprot.2012.03.017
5. Guo YS, Li XM, Ye SJ, Zhang SS (2013) Modern optical techniques provide a bright outlook for cell analysis. TrAC Trends Anal Chem 42:168–185. doi:10.1016/j.trac.2012.09.018
6. Kleparnik K, Foret F (2013) Recent advances in the development of single cell analysis—a review. Anal Chim Acta 800:12–21. doi:10.1016/j.aca.2013.09.004
7. Proefrock D, Prange A (2012) Inductively coupled plasma-mass spectrometry (ICP-MS) for quantitative analysis in environmental and life sciences: a review of challenges, solutions, and trends. Appl Spectrosc 66(8):843–868. doi:10.1366/12-06681
8. Alkilany AM, Murphy CJ (2010) Toxicity and cellular uptake of gold nanoparticles: what we have learned so far? J Nanoparticle Res 12(7):2313–2333. doi:10.1007/s11051-010-9911-8
9. Cerchiaro G, Manieri TM, Bertuchi FR (2013) Analytical methods for copper, zinc, and iron quantification in mammalian cells. Metallomics 5(10):1336–1345. doi:10.1039/c3mt00136a
10. Lobinski R, Moulin C, Ortega R (2006) Imaging and speciation of trace elements in biological environment. Biochimie 88(11):1591–1604. doi:10.1016/j.biochi.2006.10.003
11. McRae R, Bagchi P, Sumalekshmy S, Fahrni CJ (2009) In situ imaging of metals in cells and tissues. Chem Rev 109(10):4780–4827. doi:10.1021/cr900223a
12. Ortega R, Deves G, Carmona A (2009) Biometals imaging and speciation in cells using proton and synchrotron radiation X-ray

microspectroscopy. J R Soc Interface 6:649–658. doi:10.1098/rsif.2009.0166.focus
13. Ortega R (2005) Chemical elements distribution in cells. Nucl Inst Methods Phys Res B 231:218–223. doi:10.1016/j.nimb.2005.01.060
14. Qin Z, Caruso JA, Lai B, Matusch A, Becker JS (2011) Trace metal imaging with high spatial resolution: applications in biomedicine. Metallomics 3(1):28–37. doi:10.1039/c0mt00048e
15. Wu B, Becker JS (2011) Imaging of elements and molecules in biological tissues and cells in the low-micrometer and nanometer range. Int J Mass Spectrom 307(1/3):112–122. doi:10.1016/j.ijms.2011.01.019
16. Konz I, Fernandez B, Fernandez ML, Pereiro R, Sanz-Medel A (2012) Laser ablation ICP-MS for quantitative biomedical applications. Anal Bioanal Chem 403(8):2113–2125. doi:10.1007/s00216-012-6023-6
17. Becker JS, Zoriy M, Matusch A, Wu B, Salber D, Palm C (2010) Bioimaging of metals by laser ablation inductively coupled plasma mass spectrometry (LA-ICP-MS). Mass Spectrom Rev 29(1):156–175. doi:10.1002/mas.20239
18. Giesen C, Waentig L, Panne U, Jakubowski N (2012) History of inductively coupled plasma mass spectrometry-based immunoassays. Spectrochim Acta B 76:27–39. doi:10.1016/j.sab.2012.06.009
19. Hare D, Austin C, Doble P (2012) Quantification strategies for elemental imaging of biological samples using laser ablation-inductively coupled plasma-mass spectrometry. Analyst 137:1527–1537
20. Wu B, Niehren S, Becker JS (2011) Mass spectrometric imaging of elements in biological tissues by new BrainMet technique-laser microdissection inductively coupled plasma mass spectrometry (LMD-ICP-MS). J Anal At Spectrom 26(8):1653–1659. doi:10.1039/c1ja10106d
21. Nomizu T, Kaneco S, Tanaka T, Ito D, Kawaguchi H, Vallee BT (1994) Determination of calcium content in individual biological cells by inductively-coupled plasma-atomic emission-spectrometry. Anal Chem 66(19):3000–3004. doi:10.1021/ac00091a004
22. Haraguchi H, Ishii A, Hasegawa T, Matsuura H, Umemura T (2008) Metallomics study on all-elements analysis of salmon egg cells and fractionation analysis of metals in cell cytoplasm. Pure Appl Chem 80(12):2595–2608
23. Haraguchi H (2004) Metallomics as integrated biometal science. J Anal At Spectrom 19(1):5–14. doi:10.1039/B308213j
24. Li F, Armstrong DW, Houk RS (2005) Behavior of bacteria in the inductively coupled plasma: atomization and production of atomic ions for mass spectrometry. Anal Chem 77(5):1407–1413. doi:10.1021/ac049188l
25. Ho K-S, Chan W-T (2010) Time-resolved ICP-MS measurement for single-cell analysis and on-line cytometry. J Anal At Spectrom 25(7):111–1122. doi:10.1039/c002272a
26. Tsang CN, Ho KS, Sun HZ, Chan WT (2011) Tracking bismuth antiulcer drug uptake in single *Helicobacter pylori* cells. J Am Chem Soc 133(19):7355–7357. doi:10.1021/ja2013278
27. Groombridge AS, Miyashita S, Fujii S, Nagasawa K, Okahashi T, Ohata M, Umemura T, Takatsu A, Inagaki K, Chiba K (2013) High sensitive elemental analysis of single yeast cells (saccharomyces cerevisiae) by time-resolved inductively-coupled plasma mass spectrometry using a high efficiency cell introduction system. Anal Sci 29(6):597–603
28. Zheng LN, Wang M, Wang B, Chen HQ, Ouyang H, Zhao YL, Chai ZF, Feng WY (2013) Determination of quantum dots in single cells by inductively coupled plasma mass spectrometry. Talanta 116:782–787. doi:10.1016/j.talanta.2013.07.075
29. Shigeta K, Traub H, Panne U, Okino A, Rottmann L, Jakubowski N (2013) Application of a micro-droplet generator for an ICP-sector field mass spectrometer - optimization and analytical characterization. J Anal At Spectrom 28:646–656
30. Shigeta K, Koellensperger G, Rampler E, Traub H, Rottmann L, Panne U, Okino A, Jakubowski N (2013) Sample introduction of single selenized yeast cells (*Saccharomyces cerevisiae*) by micro droplet generation into ICP-sector field mass spectrometer for label free detection of trace elements. J Anal At Spectrom 28(5):637–645
31. Verboket PE, Borovinskaya O, Meyer N, Günther D, Dittrich PS (2014) A new microfluidics-based droplet dispenser for ICPMS. Anal Chem 86:6012–6018. doi:10.1021/ac501149a
32. Chen BB, Heng SJ, Peng HY, Hu B, Yu X, Zhang ZL, Pang DW, Yue X, Zhu Y (2010) Magnetic solid phase microextraction on a microchip combined with electrothermal vaporization-inductively coupled plasma mass spectrometry for determination of Cd, Hg, and Pb in cells. J Anal At Spectrom 25(12):1931–1938. doi:10.1039/c0ja00003e
33. Wang H, Wu ZK, Zhang Y, Chen BB, He M, Hu B (2013) Chip-based liquid phase microextraction combined with electrothermal vaporization-inductively coupled plasma mass spectrometry for trace metal determination in cell samples. J Anal At Spectrom 28(10):1660–1665. doi:10.1039/c3ja50223f
34. Badiei HR, Rutzke MA, Karanassios V (2002) Calcium content of individual, microscopic, (sub) nanoliter volume *Paramecium* sp. cells using rhenium-cup in-torch vaporization (ITV) sample introduction and axially viewed ICP-AES. J Anal At Spectrom 17(9):1007–1010. doi:10.1039/b203352f
35. Hamid RB (2004) Further development, optimization, and characterization of in-torch vaporization-inductively coupled plasma (ITV-ICP) spectrometry; 487 pp Avail: UMI, Order No DANQ91978 from: Diss Abstr Int, B 2004, 65(5), 2387
36. Chithrani BD, Ghazani AA, Chan WC (2006) Determining the size and shape dependence of gold nanoparticle uptake into mammalian cells. Nano Lett 6(4):662–668
37. Nativo P, Prior IA, Brust M (2008) Uptake and intracellular fate of surface-modified gold nanoparticles. ACS Nano 2(8):1639–1644. doi:10.1021/nn800330a
38. Gilbert B, Fakra SC, Xia T, Pokhrel S, Mädler L, Nel AE (2012) The fate of ZnO nanoparticles administered to human bronchial epithelial cells. ACS Nano 26;6(6):4921–4930. doi:10.1021/nn300425a
39. Drescher D, Giesen C, Traub H, Panne U, Kneipp J, Jakubowski N (2012) Quantitative imaging of gold and silver nanoparticles in single eukaryotic cells by laser ablation ICP-MS. Anal Chem 84(22):9684–9688
40. Drescher D, Zeise I, Traub H, Guttmann P, Seifert S, Büchner T, Jakubowski N, Schneider G, Kneipp J (2014) In situ Characterization of SiO2 nanoparticle biointeractions using bright silica. Adv Funct Mater 24:3765–3775. doi:10.1002/adfm.201304126
41. Wang HAO, Grolimund D, Giesen C, Borca CN, Shaw-Stewart JRH, Bodenmiller B, Gunther D (2013) Fast chemical imaging at high spatial resolution by laser ablation inductively coupled plasma mass spectrometry. Anal Chem 85(21):10107–10116. doi:10.1021/ac400996x
42. Giesen C, Wang HA, Schapiro D, Zivanovic N, Jacobs A, Hattendorf B, Schüffler PJ, Grolimund D, Buhmann JM, Brandt S (2014) Highly multiplexed imaging of tumor tissues with subcellular resolution by mass cytometry. Nat Methods. doi:10.1038/NMETH.2869
43. Jiang L, Qian J, Cai F, He S (2011) Raman reporter-coated gold nanorods and their applications in multimodal optical imaging of cancer cells. Anal Bioanal Chem 400(9):2793–2800
44. Drescher D, Kneipp J (2012) Nanomaterials in complex biological systems: insights from Raman spectroscopy. Chem Soc Rev 41(17):5780–5799
45. Hagenhoff B, Breitenstein D, Tallarek E, Möllers R, Niehuis E, Sperber M, Goricnik B, Wegener J (2012) Detection of micro- and nano-particles in animal cells by ToF-SIMS 3D analysis. Surf Interf Anal 45(1):315–319
46. Haase A, Arlinghaus HF, Tentschert J, Jungnickel H, Graf P, Mantion A, Draude F, Galla S, Plendl J, Goetz ME, Masic A, Meier W, Thünemann AF, Taubert A, Luch A (2011) Application of laser post-ionization secondary neutral mass spectrometry/time-of-flight

secondary ion mass spectrometry in nanotoxicology: visualization of nanosilver in human macrophages and cellular responses. ACS Nano 26;5(4):3059–3068. doi:10.1021/nn200163w
47. Managh AJ, Edwards SL, Bushell A, Wood KJ, Geissler EK, Hutchinson JA, Hutchinson RW, Reid HJ, Sharp BL (2013) Single cell tracking of gadolinium labeled CD4(+) T cells by laser ablation inductively coupled plasma mass spectrometry. Anal Chem 85(22): 10627–10634. doi:10.1021/ac4022715
48. Schwarz G, Mueller L, Beck S, Linscheid MW (2014) DOTA-based metal labels for protein quantification: a review. J Anal At Spectrom 29(2):221–233
49. Waentig L, Jakubowski N, Hardt S, Scheler C, Roos PH, Linscheid MW (2012) Comparison of different chelates for lanthanide labeling of antibodies and application in a Western blot immunoassay combined with detection by laser ablation (LA-) ICP-MS. J Anal At Spectrom 27:9
50. Bendall SC, Nolan GP, Roederer M, Chattopadhyay PK (2012) A deep profiler's guide to cytometry. Trends Immunol 33(7):323–332
51. Lou XD, Zhang GH, Herrera I, Kinach O, Ornatsky O, Baranov V, Nitz M, Winnik MA (2007) Polymer-based elemental tags for sensitive bioassays. Angew Chem Int Ed 46(32):6111–6114
52. Tanner SD, Bandura DR, Ornatsky O, Baranov VI, Nitz M, Winnik MA (2008) Flow cytometer with mass spectrometer detection for massively multiplexed single-cell biomarker assay. Pure Appl Chem 80(12):2627–2641
53. Terenghi M, Elviri L, Careri M, Mangia A, Lobinski R (2009) Multiplexed determination of protein biomarkers using metal-tagged antibodies and size exclusion chromatography-inductively coupled plasma mass spectrometry. Anal Chem 81(22):9440–9448. doi:10.1021/Ac901853g
54. de Bang TC, Pedas P, Schjoerring JK, Jensen PE, Husted S (2013) Multiplexed quantification of plant thylakoid proteins on Western blots using lanthanide-labeled antibodies and laser ablation inductively coupled plasma mass spectrometry (LA-ICP-MS). Anal Chem 85(10):5047–5054. doi:10.1021/ac400561q
55. Mueller L, Mairinger T, Hermann G, Koellensperger G, Hann S (2014) Characterization of metal-tagged antibodies used in ICP-MS-based immunoassays. Anal Bioanal Chem 406(1):163–169
56. Bandura DR, Baranov VI, Ornatsky OI, Antonov A, Kinach R, Lou XD, Pavlov S, Vorobiev S, Dick JE, Tanner SD (2009) Mass cytometry: technique for real time single cell multitarget immunoassay based on inductively coupled plasma time-of-flight mass spectrometry. Anal Chem 81(16):6813–6822. doi: 10.1021/Ac901049w
57. Ornatsky OI, Lou X, Nitz M, Schaefer S, Sheldrick WS, Baranov VI, Bandura DR, Tanner SD (2008) Study of Cell Antigens and Intracellular DNA by Identification of element-containing labels and metallointercalators using inductively coupled plasma mass spectrometry. Anal Chem 80(7):2539–2547
58. Bendall SC, Simonds EF, Qiu P, Amir EAD, Krutzik PO, Finck R, Bruggner RV, Melamed R, Trejo A, Ornatsky OI, Balderas RS, Plevritis SK, Sachs K, Pe'er D, Tanner SD, Nolan GP (2011) Single-cell mass cytometry of differential immune and drug responses across a human hematopoietic continuum. Science 332(6030):687–696. doi:10.1126/science.1198704
59. Qiu P, Simonds EF, Bendall SC, Gibbs KD, Bruggner RV, Linderman MD, Sachs K, Nolan GP, Plevritis SK (2011) Extracting a cellular hierarchy from high-dimensional cytometry data with SPADE. Nat Biotechnol 29(10):886–891. doi:10.1038/nbt.1991
60. Bodenmiller B, Zunder ER, Finck R, Chen TJ, Savig ES, Bruggner RV, Simonds EF, Bendall SC, Sachs K, Krutzik PO, Nolan GP (2012) Multiplexed mass cytometry profiling of cellular states perturbed by small-molecule regulators. Nat Biotechnol 30(9):858–U889. doi:10.1038/nbt.2317
61. Zivanovic N, Jacobs A, Bodenmiller B (2013) A Practical Guide to Multiplexed Mass Cytometry
62. Behbehani GK, Bendall SC, Clutter MR, Fantl WJ, Nolan GP (2012) Single-cell mass cytometry adapted to measurements of the cell cycle. Cytometry A 81A(7):552–566. doi:10.1002/cyto.a.22075
63. Fienberg HG, Simonds EF, Fantl WJ, Nolan GP, Bodenmiller B (2012) A platinum-based covalent viability reagent for single-cell mass cytometry. Cytometry A 81A(6):467–475. doi:10.1002/cyto.a.22067
64. Mingueneau M, Kreslavsky T, Gray D, Heng T, Cruse R, Ericson J, Bendall S, Spitzer M, Nolan G, Kobayashi K, von Boehmer H, Mathis D, Benoist C, Best AJ, Knell J, Goldrath A, Jojic V, Koller D, Shay T, Regev A, Cohen N, Brennan P, Brenner M, Kim F, Rao TN, Wagers A, Rothamel K, Ortiz-Lopez A, Bezman NA, Sun JC, Min-Oo G, Kim CC, Lanier LL, Miller J, Brown B, Merad M, Gautier EL, Jakubzick C, Randolph GJ, Monach P, Blair DA, Dustin ML, Shinton SA, Hardy RR, Laidlaw D, Collins J, Gazit R, Rossi DJ, Malhotra N, Sylvia K, Kang J, Fletcher A, Elpek K, Bellemare-Pelletier A, Malhotra D, Turley S, Immunological Genome C (2013) The transcriptional landscape of alpha beta T cell differentiation. Nat Immunol 14(6):619–632. doi:10.1038/ni.2590
65. De J, Shah NP, Ballentine CT, Maecker HT (2013) High-dimensional mass cytometry analysis reveals differential STAT activation in cellular subsets of chronic myelogenous leukemia. Lab Investig 93: 441A–441A
66. Lee D, Martinez S, Senyukov V, Emanuel P, Liu YY (2013) High-dimension single-cell mass cytometry and colony-forming assays to determine the susceptibility of juvenile myelomonocytic leukemia to NK cell immunotherapy. Pediatr Blood Cancer 60:S41–S41
67. Fisher DAC, Simonds EF, Behbehani GK, Nolan GP, Bendall SC, Oh ST (2012) Single cell mass cytometry of dysregulated signaling networks in myeloproliferative neoplasms and secondary acute myeloid leukemia. Blood 120 (21):Meeting Abstract 703
68. Fragiadakis G, Gaudilliere B, Angst M, Nolan G (2013) Single cell mass cytometry of human peripheral blood reveals an endogenous immune response to surgical trauma. J Immunol 190:Meeting Abstract P1144
69. Wang LL, Abbasi F, Ornatsky O, Cole KD, Misakian M, Gaigalas AK, He HJ, Marti GE, Tanner S, Stebbings R (2012) Human CD4(+) lymphocytes for antigen quantification: characterization using conventional flow cytometry and mass cytometry. Cytometry A 81A(7): 567–575. doi:10.1002/cyto.a.22060
70. Sen N, Mukherjee G, Bendall SC, Sen A, Jager A, Sung P, Nolan GP, Johnstone I, Arvin AM (2013) Multiparametric high dimensional analysis of normal and VZV infected human tonsil T cells at a single cell resolution by mass cytometry. Cytokine 63(3):298–298. doi:10.1016/j.cyto.2013.06.236
71. Newell EW, Sigal N, Nair N, Kidd BA, Greenberg HB, Davis MM (2013) Combinatorial tetramer staining and mass cytometry analysis facilitate T-cell epitope mapping and characterization. Nat Biotechnol 31(7):623–629. doi:10.1038/nbt.2593
72. Lin DX, Piard-Ruster K, Esquivel C, Martinez O, Maecker H (2013) T cell responses to Epstein-Barr virus infections in pediatric organ transplant recipients. J Immunol 190
73. Spitzer M, Hotson A, Bendall S, Engleman E, Nolan G (2013) Systematically defining murine immunity at the phenotypic and functional levels via mass cytometry. J Immunol 190:Meeting Abstract P3283
74. Horowitz A, Strauss-Albee DM, Leipold M, Kubo J, Nemat-Gorgani N, Dogan OC, Dekker CL, Mackey S, Maecker H, Swan GE, Davis MM, Norman PJ, Guethlein LA, Desai M, Parham P, Blish CA (2013) Genetic and environmental determinants of human NK cell diversity revealed by mass cytometry. Sci Transl Med 5(208)
75. Piard-Ruster K, Krams S, Esquivel C, Martinez O (2013) Cytometry time of flight (CyTOF) analysis of Epstein-Barr virus-specific T cells in pediatric liver transplant recipients. Am J Transplant 13:287–287
76. Agnetti G (2012) Mass spectrometry goes with the flow: mass cytometry and its potentials in regenerative medicine. Circ Cardiov Genet 5(3):379–380. doi:10.1161/circgenetics.112.963694

77. Bjornson ZB, Nolan GP, Fantl WJ (2013) Single-cell mass cytometry for analysis of immune system functional states. Curr Opin Immunol 25(4):484–494
78. Giesen C, Waentig L, Mairinger T, Drescher D, Kneipp J, Roos PH, Panne U, Jakubowski N (2011) Iodine as an elemental marker for imaging of single cells and tissue sections by laser ablation inductively coupled plasma mass spectrometry. J Anal At Spectrom 26(11):2160–2165. doi:10.1039/c1ja10227c
79. Waentig L, Jakubowski N, Hayen H, Roos PH (2011) Iodination of proteins, proteomes, and antibodies with potassium triodide for LA-ICP-MS based proteomic analyses. J Anal At Spectrom 26(8): 1610–1618. doi:10.1039/c1ja10090d
80. Becker JS, Gorbunoff A, Zoriy M, Izmer A, Kayser M (2006) Evidence of near-field laser ablation inductively coupled plasma mass spectrometry (NF-LA-ICP-MS) at nanometre scale for elemental and isotopic analysis on gels and biological samples. J Anal At Spectrom 21(1):19–25. doi:10.1039/B514401a
81. Angelo M, Bendall SC, Finck R, Hale MB, Hitzman C, Borowsky AD, Levenson RM, Lowe JB, Liu SD, Zhao S, Natkunam Y, Nolan GP (2014) Nat Med 20:436–442